

**SatBałtyk – A Baltic
environmental satellite
remote sensing system
– an ongoing project
in Poland. Part 2:
Practical applicability and
preliminary results***

doi:10.5697/oc.53-4.925
OCEANOLOGIA, 53 (4), 2011.
pp. 925–958.

© Copyright by
Polish Academy of Sciences,
Institute of Oceanology,
2011.

KEYWORDS
Marine optics in Poland
Satellite monitoring
Remote sensing system
Baltic Sea

BOGDAN WOŹNIAK^{1,3,*}, KATARZYNA BRADTKE²,
MIROŚLAW DARECKI¹, JERZY DERA¹,
JOANNA DUDZIŃSKA-NOWAK⁴, LIDIA DZIERZBICKA-GŁOWACKA¹,
DARIUSZ FICEK³, KAZIMIERZ FURMAŃCZYK⁴,
MAREK KOWALEWSKI², ADAM KRĘŻEL²,
ROMAN MAJCHROWSKI³, MIROŚLAWA OSTROWSKA¹,
MARCIN PASZKUTA², JOANNA STOŃ-EGIERT¹,
MAŁGORZATA STRAMSKA^{1,4}, TOMASZ ZAPADKA³

¹ Institute of Oceanology, Polish Academy of Sciences,
Powstańców Warszawy 55, Sopot 81–712, Poland;

e-mail: wozniak@iopan.gda.pl

*corresponding author

² Institute of Oceanography, University of Gdańsk,
al. Marszałka Piłsudskiego 46, Gdynia 81–378, Poland

³ Institute of Physics, Pomeranian University in Słupsk,
Arciszewskiego 22B, Słupsk 76–200, Poland

⁴ Institute of Marine and Coastal Sciences, University of Szczecin,
Mickiewicza 18, Szczecin 70–383, Poland

Received 23 August 2011, revised 25 October 2011, accepted 1 November 2011.

* This work was carried out within the framework of the SatBałtyk project funded by the European Union through European Regional Development Fund, (contract No. POIG.01.01.02-22-011/09 entitled ‘The Satellite Monitoring of the Baltic Sea Environment’) and also as a part of IO PAS’s statutory research.

The paper was presented in part at the 6th International Conference ‘Current Problems in the Optics of Natural Waters’, St. Petersburg, Russia, 6–10 September 2011.

The complete text of the paper is available at <http://www.iopan.gda.pl/oceanologia/>

Abstract

This paper is the second part of the description of the first stage of the SatBałtyk project's implementation. Part 1 (Woźniak et al. 2011, in this issue) presents the assumptions and objectives of SatBałtyk and describes the most important stages in the history of our research, which is the foundation of this project. It also discusses the operation and general structure of the SatBałtyk system. Part 2 addresses various aspects of the practical applicability of the SatBałtyk Operational System to Baltic ecosystem monitoring. Examples are given of the Baltic's characteristics estimated using the preliminary versions of the algorithms in this Operational System. At the current stage of research, these algorithms apply mainly to the characteristics of the solar energy influx and the distribution of this energy among the various processes taking place in the atmosphere-sea system, and also to the radiation balance of the sea surface, the irradiance conditions for photosynthesis and the condition of plant communities in the water, sea surface temperature distributions and some other marine phenomena correlated with this temperature. Monitoring results obtained with these preliminary algorithms are exemplified in the form of distribution maps of selected abiotic parameters of the Baltic, as well as structural and functional characteristics of this ecosystem governed by these parameters in the Baltic's many basins. The maps cover practically the whole area of the Baltic Sea. Also given are results of preliminary inspections of the accuracy of the magnitudes shown on the maps. In actual fact, the errors of these estimates are relatively small. The further practical application of this set of algorithms (to be gradually made more specific) is therefore entirely justified as the basis of the SatBałtyk system for the effective operational monitoring of the state and functioning of Baltic ecosystems. This article also outlines the plans for extending SatBałtyk to include the recording of the effects and hazards caused by current and expected storm events in the Polish coastal zone.

1. Introduction

The present article (Part 2) brings to a close the summary of the results of the first year and a half of SatBałtyk's implementation. Planned to run for 5 years, the project is to end on 31 December 2014. The final result of the project is to be the creation and setting in motion of the SatBałtyk Operational System (SBOS¹), the aim of which is to monitor effectively and comprehensively the state of the Baltic Sea environment using remote sensing techniques. As already explained in Part 1 (see Woźniak et al. 2011, in this issue), the SatBałtyk project is being realized by the SatBałtyk Scientific Consortium, specifically appointed for this purpose, which associates four scientific institutions: the Institute of Oceanology PAN in Sopot – coordinator, the University of Gdańsk

¹The principal abbreviations and symbols used can be found in the Annexes 1 and 2.

(Institute of Oceanography), the Pomeranian University in Słupsk (Institute of Physics) and the University of Szczecin (Institute of Marine Sciences).

In Part 1 of this two-part paper we described the assumptions and objectives of the SatBałtyk project and presented a resumé of the history of the research done by its authors, who laid the foundations for this project. We also described the way in which SatBałtyk functions and the scheme of its overall operational system. In Part 2 we discuss various aspects of the practical applicability of SBOS to the monitoring of the Baltic ecosystem. With this in mind we present some examples of the test measurements of the various characteristics of the Baltic obtained using the current version of SBOS, including algorithms and models that are still in an unfinished state. They are mainly distribution maps for the whole Baltic of crucial abiotic parameters of the marine environment, and of a number of structural and functional properties of this sea dependent on these parameters. These magnitudes are significant with regard to the study of 5 sets of phenomena and processes, some of the most important themes in contemporary marine science:

1. The influx and distribution of the solar radiation energy consumed during various processes in the atmosphere-sea system.
2. The radiation balance of the sea surface.
3. The optical conditions in which photosynthesis of organic matter takes place and the condition of marine plant communities.
4. Distributions of sea surface temperature (SST) and the links between this temperature and various phenomena occurring in the sea.
5. Hazards and effects due to storm states in the coastal zone of the sea.

The point of presenting the first two of these sets of processes is to demonstrate that with the aid of remote sensing techniques it is possible to effectively (on a large scale – the whole Baltic and even the whole Earth) monitor all the processes, stimulated by the Sun's life-giving radiation, governing the existence and functioning of ecosystems and shaping the Earth's climate. A simplified scheme of these processes is shown in Figure 1: it illustrates these processes in two phases, outlined below.

Phase 1 (the left-hand side of Figure 1): the influx of solar radiation energy and the distribution of this energy among various processes taking place in the atmosphere-sea system. These are: the absorption and scattering of solar radiation in the atmosphere; the transmission through the atmosphere of this radiation and its reflection from the sea surface; its diffusion down into the water, where it is absorbed by water molecules and the dissolved and suspended, organic and inorganic substances it contains. Separate, detailed treatment is given to the absorption of this radiation by

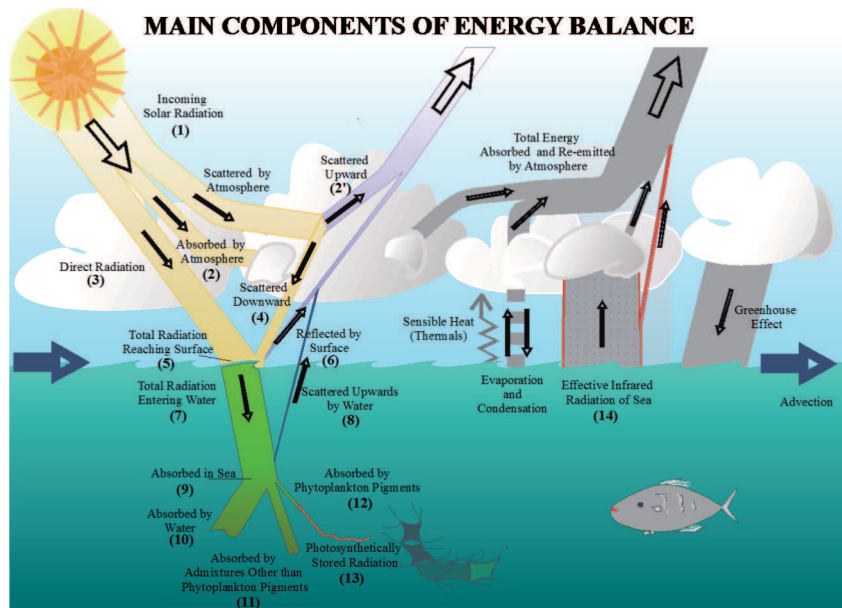


Figure 1. The main elements of the energy balance in the atmosphere–sea system (adapted from Woźniak et al. 2003b)

phytoplankton pigments and the partial utilization of this absorbed energy for the photosynthesis of organic matter, that is the supply to the marine ecosystem of the energy its needs in order to be able to function.

Phase 2 (the right-hand side of Figure 1): the formation of an upward, water-leaving radiation flux, which is equally important in the shaping of the Earth’s climate. This flux consists of two components: short-wave radiation and long-wave radiation. The former consists of sunlight backscattered as a result of multiple scattering in the atmosphere and in the sea, and upward reflection from the sea surface. The latter is thermal radiation, generated, for example, in the sea water and in the atmosphere as they warm up following the absorption of solar radiation and other energy transformations in the sea-atmosphere system.

Most of the processes depicted in Figure 1 are quantitatively exemplified in this paper by measurements made in the Baltic. This was done using the component algorithms of SBOS based solely on satellite data, or such data complemented by hydrometeorological and other data supplied by the relevant services. The various magnitudes governing or describing processes taking place in the sea and in the atmosphere over the sea are illustrated in section 2 (subsections 2.1, 2.2 and 2.3) in the form of maps showing their distribution in the Baltic Sea region.

Another objective of this article is to demonstrate the possibilities of using satellite data for determining the parameters characterizing the optical conditions of marine photosynthesis. These parameters are the depth of the euphotic zone and the photosynthetic index of the basin, which in a way also define the physiological state (including the condition) of the natural plant communities growing there. In detail, they are the maximum possible assimilation number, the maximum quantum efficiency of photosynthesis and the ‘factor of non-photosynthetic pigments’. Examples of the spatial distribution of these physiological characteristics of plant communities and the optical conditions in the Baltic will be found in subsection 2.4.

An important partial objective of our work to date on this project has been

1. on the one hand to improve the direct remote sensing of SST, or in the case of overcast skies, to complement SSTs using a forecasting model,
2. and on the other hand, to check and demonstrate the possibilities of using SST distribution maps of the Baltic for identifying certain complex SST-correlated phenomena taking place in this sea, e.g. upwelling events.

Examples of spatial SST distributions determined with the aid of our algorithms and the various complex phenomena identified in the Baltic on their basis are presented in subsection 2.5.

In this initial period of the realization of SatBałtyk that we are describing here, we have also been working on the documentation of the effects and hazards in the coastal zone, mainly of the southern Baltic, due to current and expected storm states. To this end we intend to utilize data from the SatBałtyk prognostic models, with satellite data being treated as auxiliary information. In the future this will form an extension to the existing early storm-warning system developed during the 7th Framework Programme of the MICORE Project – Morphological Impacts and Coastal Risk Induced by Extreme Storm Events (www.micore.eu). The assumptions underpinning the development of this early-warning system are described briefly in section 3.

2. Validation of the SatBałtyk Operational System: some examples

The validations of the preliminary versions of SBOS algorithms, exemplified in subsections 2.1 to 2.4, and the DESAMBEM diagnostic subsystem, will be presented in the form of distribution maps of selected environmental characteristics, namely, the optical characteristics of the atmosphere above the Baltic Sea, and some structural and functional characteristics of the

ecosystem governed by these parameters in the sea's many basins. The maps cover practically the entire Baltic region. In order to make meaningful comparisons of the spatial distributions of these characteristics, most of the maps refer to their state at the same time, i.e. the situation in the hours around noon on 24 April 2011. The relevant calculations using the DESAMBEM diagnostic algorithms were carried out on the basis of input data consisting of two kinds of empirical data: 1) remote sensing data from that day acquired from various satellite systems, including MODIS (AQUA), SEVIRI (METEOSAT 9) and AVHRR (NOAA 17, 18, 19) sensors; 2) meteorological data, that is, water vapour pressure, atmospheric pressure at the sea level, sea surface temperature SST. These latter data were obtained from data generated by the operational meteorological model at the ICM Interdisciplinary Centre for Mathematical and Computational Modelling, Warsaw University – <http://www.icm.edu.pl/eng/>.

Subsection 2.5 outlines the benefits of using prognostic models for estimating SST distributions in areas with overcast skies and for various marine phenomena associated with this temperature. For this purpose the situation at the end of April 2009 was examined, the relevant calculations being carried out using not one but both SBOS subsystems, i.e. the DESAMBEM Diagnostic System and the BALTFOS Forecasting System. The input data for estimating the SST of overcast areas of the sea were the SST values in cloudless areas derived from thermal infrared radiances remotely recorded by an AVHRR sensor (TIROS-N/NOAA) on 28 and 29 April 2009.

Note that below we restrict ourselves to presenting the results of the calculations, without giving details of the algorithms or the mathematical models used to perform them: they would make this article too unwieldy, and in any case some of them have already been published (see References). That is why we now present only the most essential information characterizing the progress of this modelling.

2.1. The influx of solar radiation through the atmosphere to the sea surface and its attenuation in the atmosphere

The first stage in the driving by the Sun's life-giving radiation of all the processes governing the existence and functioning of the Earth's ecosystems and its climate takes place in the atmosphere. The processes taking place there determine what fraction of the energy of this radiation entering the upper layers of the atmosphere actually reaches the Earth's surface, and in our specific case, the Baltic Sea surface. They are the complex processes of absorption and scattering of the photons contained in this incoming solar radiation (see flux (1) in Figure 1). A significant proportion of this radiation

is thus absorbed in the atmosphere (flux (2) in Figure 1) or, as a result of multiple scattering, changes its direction of propagation and is redirected back into space (flux (2') in Figure 1), and only a part ultimately reaches the sea surface (flux (5) in Figure 1). Figure 2 shows a simplified diagram of these processes, leading to the attenuation of the solar radiation flux entering the Earth's atmosphere, from its initial value at the top of the atmosphere to its diminished value at the sea surface. For calculating the reduction in the power of this radiation as a result of its passage through the atmosphere we usually use the simplified radiation transfer equation. In Figure 2 we distinguish three stages in the influx of solar radiation to the sea surface, according to which we carry out calculations. In the first stage we define the downward irradiance $E_{\downarrow OA}$ at the top of the atmosphere (block 1 in Figure 2), which is governed directly by the solar radiation flux entering the Earth's atmosphere. This flux reaching the top of the atmosphere, averaged over time, is known as the Solar Constant (see e.g. Neckel & Labs 1981, Gueymard 2004, Darula et al. 2005); the instantaneous values of the downward irradiance at the top of the atmosphere $E_{\downarrow OA}$, associated with the Solar Constant, depend on the Sun's position in the sky, and on the distance at the instant of measuring between the Earth and the Sun in its elliptical orbit around the Sun. These instantaneous values of $E_{\downarrow OA}$ are calculated from basic astronomical formulae (e.g. Spencer 1971; see also Krężel 1985, Dera & Woźniak 2010) on the basis of the geographical

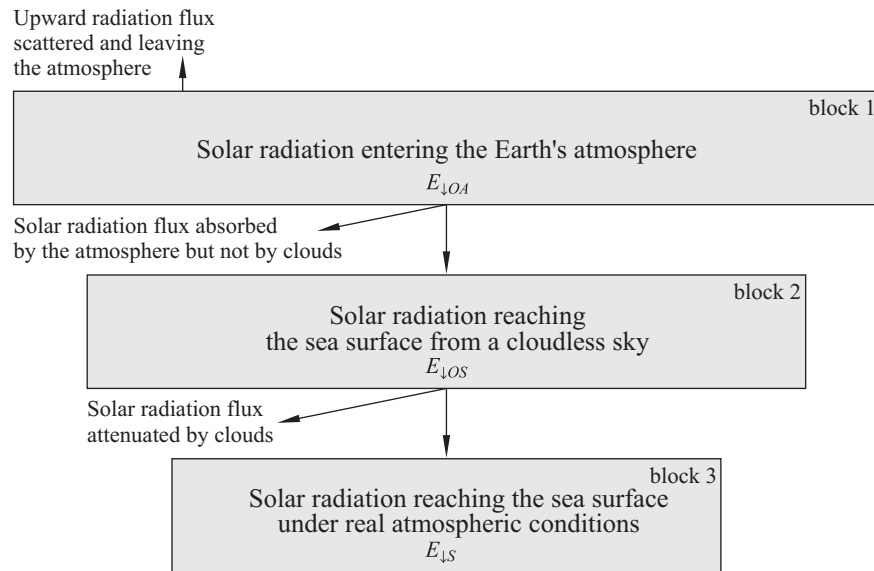


Figure 2. Diagram showing the sequence of stages for calculating the transfer of solar radiation through the atmosphere to the sea surface

coordinates of the measuring station and time (the day number of the year and the time of day).

The second stage in these calculations yields the downward irradiance $E_{\downarrow OS}$ of the solar radiation reaching the sea surface from a cloudless sky; here, the influence of clouds on this flux is neglected (Block 2 in Figure 2). What is taken into consideration is the reduction in downward irradiance due to the attenuation of the solar radiation flux on its passage through the atmosphere by scattering and absorption by atmospheric components such as water vapour, ozone and aerosols. These calculations are performed on the basis of more complex models of optical processes taking place in a cloudless atmosphere (see e.g. Bird & Riordan 1986, Krężel 1997, Woźniak et al. 2008). As already mentioned, they take account of the effects of various constant and variable components of the atmosphere on its optical properties, including the variable contents of different types of atmospheric aerosols. These are responsible for the greatest changes in the transmittance of the radiation flux in the atmosphere with the exception of the effect of clouds on this flux.

Finally, the third stage in these calculations involves determining the values of the real downward irradiance at the sea surface $E_{\downarrow S}$, associated with the solar radiation flux reaching the sea surface under real atmospheric conditions, that is, when the real states of atmospheric cloudiness are taken into consideration (besides the solar zenith angle; Block 3 in Figure 2). Changes in cloud coverage are responsible in the highest degree for changes in the transmittance of the radiation flux through the atmosphere. For these calculations we use an optical model developed by our team, which contains relationships for estimating the transmittance of solar radiation in a real terrestrial atmosphere, completely or partly covered by cloud (see Woźniak et al. 2003b, 2008, Krężel et al. 2008, Krężel & Paszkuta 2011).

Calculated in accordance with the above scheme, the magnitudes characterizing the solar radiation flux through the atmosphere to the Baltic Sea surface and the parameters governing its attenuation in the atmosphere, are illustrated in map form in Figure 3. The maps in Figures 3a to 3c quantitatively illustrate the reduction in the solar radiation flux diffusing through the atmosphere to the sea surface and show the relevant irradiance distributions in the Baltic area over practically the whole spectral range reaching the sea surface (strictly speaking the wavelength interval 300–4000 nm). These are therefore the distributions of the following values: the downward irradiance of a horizontal plane at the top of the atmosphere $E_{\downarrow OA}$ (Figure 3a); the downward irradiance at the sea surface of solar radiation reaching the sea surface through a real atmosphere but neglecting the effect

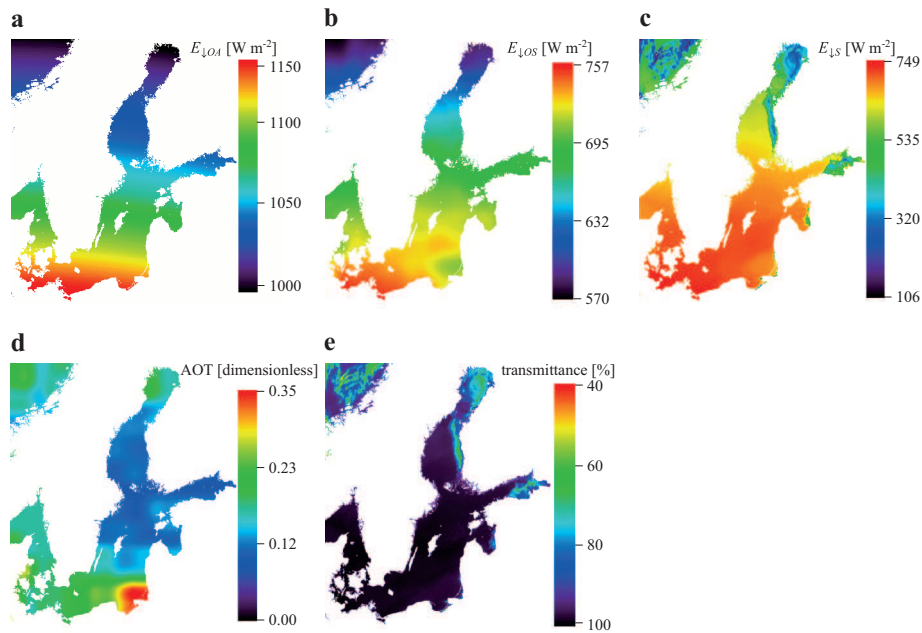


Figure 3. Examples of the remotely determined maps of the Baltic Sea on 24 April 2011 at 11:00 UTC, showing distributions of the downward irradiance associated with the solar radiation flux diffusing through the atmosphere to the sea surface, and distributions of the optical thickness of aerosols and of the downward irradiance transmittance through clouds.

- Downward irradiance in the 300–4000 nm spectral range reaching the top of the atmosphere.
- Downward irradiance in the 300–4000 nm spectral range reaching the sea surface (under real conditions but neglecting the effect of clouds).
- Downward irradiance in the 300–4000 nm spectral range reaching the sea surface under real cloudiness conditions, defined on the basis of SEVIRI data (the HRV channel).
- The aerosol optical thickness of the atmosphere (dimensionless) in the Baltic Sea region defined on the basis of AVHRR data (0.64 μm channel).
- Downward irradiance transmittance through clouds over the Baltic, defined on the basis of SEVIRI data

of clouds $E_{\downarrow OS}$ (Figure 3b), and the downward irradiance at the sea surface under real conditions, that is, the effect of cloudiness is taken into account during the determination of $E_{\downarrow S}$ (Figure 3c). The other maps (Figures 3d, 3e) show distributions of the two most important optical properties of the atmosphere, i.e. those that most strongly differentiate the surface irradiance in various parts of the Baltic Sea. The first of these properties is the aerosol optical thickness of the atmosphere (Figure 3d), which is the principal factor

reducing the downward irradiance from $E_{\downarrow OA}$ to $E_{\downarrow OS}$. The second property is the downward irradiance transmittance through clouds (Figure 3e), which quantifies the reduction in the downward irradiance at the sea surface due to clouds present in the sky at the time and site of measurement from $E_{\downarrow OS}$ to $E_{\downarrow S}$.

Characterizing the solar radiation influx through the atmosphere to the Baltic Sea surface and the parameters attenuating this irradiance in the atmosphere, the maps in Figure 3 merely illustrate certain cases of such processes. They are typical of the hours around noon on sunny spring or summer days, when the sky is cloudless or only slightly cloudy (there are clouds over only small areas of the sea). In this particular case (11:00 UTC on 24 April 2011) the irradiance transmittance by clouds over most of the Baltic was equal to or nearly 100%. It has to be borne in mind, however, that on most days in the Baltic Sea region at different times of the year, but especially in autumn and winter, the sky is often overcast. As a result, the real irradiance during a day, even around noon, is usually very much lower and may vary spatially to a great extent. Evidence for this is provided by the results of earlier studies of the daily irradiance at the Baltic surface in different seasons, carried out in the traditional manner, i.e. without the use of satellites, (e.g. Rozwadowska & Isemer 1998, Rozwadowska 2004, 2007, Krężel et al 2008, Keevallik & Loitjävrv 2010, Kowalczyk et al. 2010, see also the review by Dera & Woźniak 2010) and also by the results of the numerous studies we have started, using the remote sensing methodology described here.

2.2. The propagation of sunlight in the Baltic and its distribution among various processes

The next stage in the sunlight-driven existence and functioning of the Earth's ecosystems (here: marine ecosystems) and climate are the processes taking place in and around the sea-atmosphere interface, and then within the sea itself. Figure 1 shows that most of the solar radiation reaching the sea surface (flux (5)) is transmitted across the surface into the water (see flux (7) – total radiation entering the water), and some is reflected from this surface (flux (6) – radiation reflected by the surface) back into the atmosphere. The flux (7) then diffuses² down into the water. There it is partially backscattered, and some of this backscattered radiation may

²By the diffusion of radiation in the sea we understand the propagation of this radiation flux down into the water and the accompanying absorption and multiple scattering of photons, reducing the amount of radiation with increasing depth and also the formation of so-called diffusional radiation, i.e. radiance, which is scattered in all directions, including backwards, up to the surface.

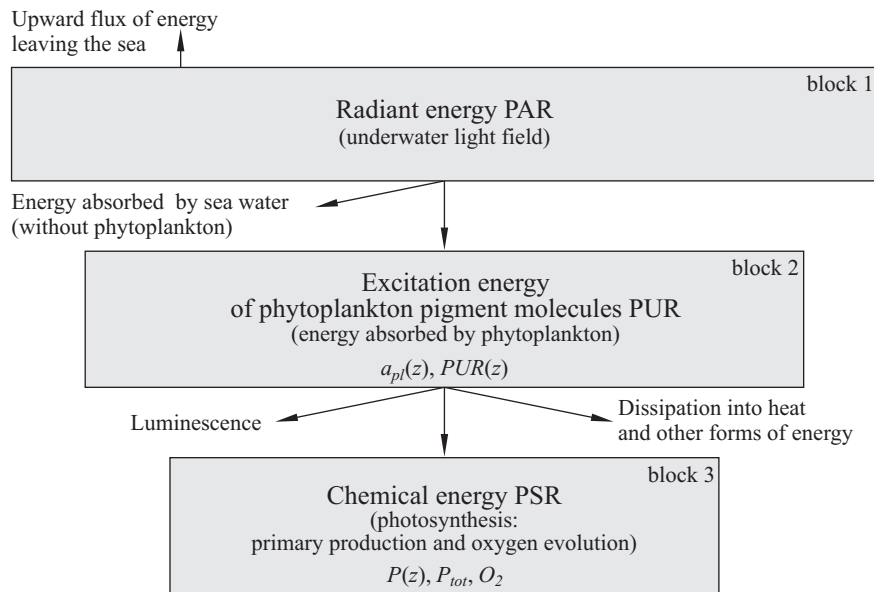


Figure 4. Diagram showing the stages of the distribution, quantitative reduction and utilization of solar radiation in the PAR spectral range (ca 400–700 nm) reaching the sea surface in various processes in the water, especially its utilization as the energy driving the ecosystem via the photosynthesis of organic matter PSR (adaptation after Woźniak 1985)

return to the atmosphere (flux (8) – radiation scattered upwards by the sea water), but most is absorbed by the components of sea water (flux (9) – radiation absorbed in the sea). Flux (9) consists of three components. Two of these are the radiation absorbed by water molecules (flux (10)) and that absorbed by the organic/inorganic substances dissolved/suspended in the water (flux (11) – the radiation absorbed by admixtures other than phytoplankton pigments). We give separate and detailed treatment to the third component of this absorption, namely, the radiation absorbed by phytoplankton pigments (PUR³) and the partial utilization of this absorbed energy for the photosynthesis (i.e. primary production) of organic matter in the sea (flux (13) – PSR⁴). In other words, this part of the energy utilized in photosynthesis supplies marine ecosystems with the energy essential for their functioning. Figure 4 shows a diagram of this energy supply in marine ecosystems. As one might guess, the mathematical description of this problem, enabling the quantitative estimation of the magnitudes

³Photosynthetically Utilized Radiation.

⁴Photosynthetically Stored Radiation.

characterizing this process, is extremely complicated. This is because we are dealing here with two not quite complete energy transformations (the absorption of radiation and photosynthesis), which are governed by various environmental factors in an exceedingly complex manner. These energy transformations take place between the following three forms of energy:

- (block 1) – PAR⁵ – the radiant energy in the ca 400–700 nm spectral range, contained in the underwater light field, part of which as a result of absorption is transformed into the excitation energy of phytoplankton pigments PUR; another part is lost due to absorption by other components of sea water and yet more is re-emitted to the atmosphere as a consequence of the multiple scattering of the light in the sea;
- (block 2) – PUR – the excitation energy of phytoplankton pigments, i.e. the part of PAR absorbed by those pigments. Photosynthesis converts some of this light energy into chemical energy. Most, however, is dissipated in non-radiant processes (converted directly into heat) or manifests itself in various forms of luminescence (mainly the fluorescence of chlorophyll *a*);
- (block 3) – PSR – the chemical energy of intramolecular bonds produced as a result of the photosynthesis of the organic matter of phytoplankton, is formed from part of PUR. As we know, this is ‘nourishment’ for the whole marine ecosystem.

We solved the entire problem, outlined above, of the quantitative description of the energy supply to marine ecosystems, especially that of the Baltic Sea, by deriving the general, comprehensive, semi-empirical ‘light – marine photosynthesis’ mathematical model (see Woźniak et al. 2003a, Ficek et al. 2003), and complementing this general model with a series of detailed models, worked out specially for the Baltic Sea, of light-driven optical and biological processes (see Majchrowski et al. 2007, Ostrowska et al. 2007, Woźniak et al. 2007a,b). With the mathematical apparatus based on these models, the characteristics of sunlight in the Baltic and the distribution of its energy among various processes, including photosynthesis, can be estimated from the remotely sensed input data for these models. This is the foundation of the DESAMBEM diagnostic algorithm (Woźniak et al. 2008, Darecki et al. 2008) used in SBOS for calculating the results we are presenting in this paper (see Figure 5).

⁵Photosynthetically Available Radiation.

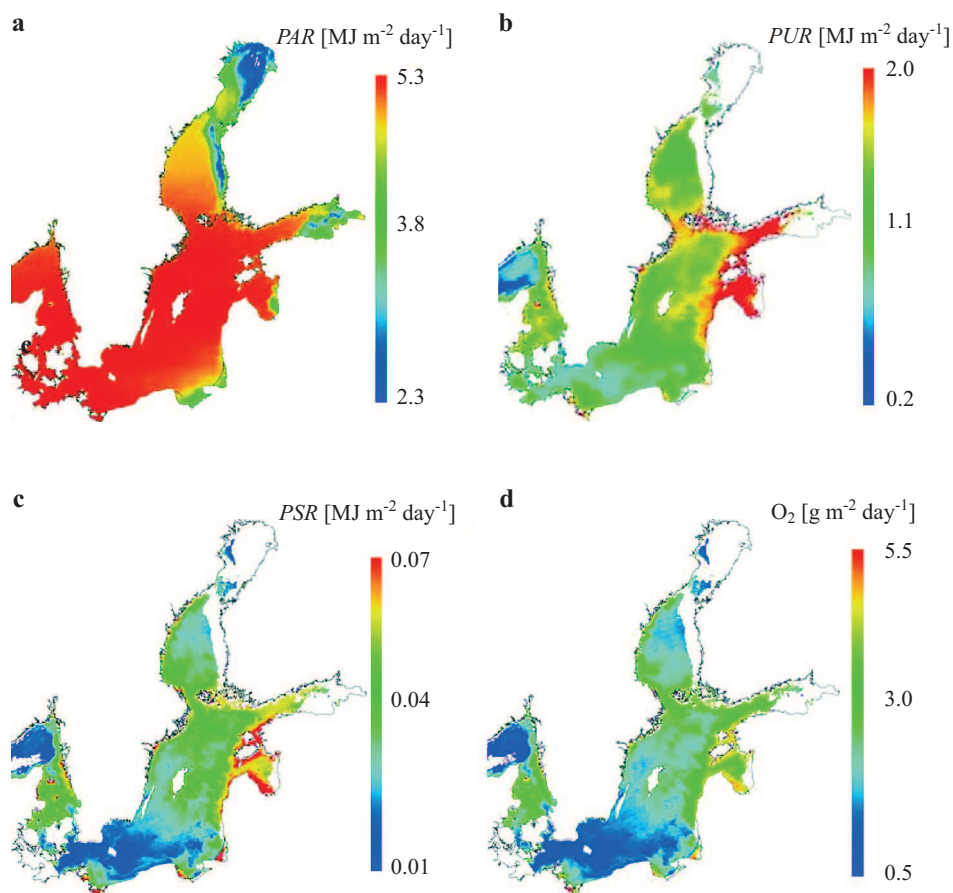


Figure 5. Example maps of remotely sensed distributions of 4 quantities in the Baltic Sea on April 24 2011: the daily doses of Photosynthetically Available Radiation (400–700 nm), PAR (a); the Photosynthetically Utilized Radiation (the excitation energy of marine phytoplankton pigments is equal to the energy of the radiation absorbed by these pigments), PUR (b); the Photosynthetically Stored Radiation (the energy incorporated into the ecosystem, that is, primary production in energy units), PSR (c); the daily quantity of oxygen O₂ released during photosynthesis in the Baltic (d)

Figure 5 illustrates the distributions of the various forms of solar energy arriving during the day time at the Baltic Sea surface and thereafter incorporated into the ecosystem via the photosynthesis of phytoplankton. They are the photosynthetically available solar radiation energy (400–700 nm) PAR (Figure 5a), the excitation energy of marine phytoplankton pigments, equal to the energy of the radiation absorbed by these pigments – PUR (Figure 5b), and the energy incorporated into the ecosystem as

primary production, that is, the Photosynthetically Stored Radiation (PSR) (Figure 5c). Finally, Figure 5d shows a map of the quantity of oxygen O_2 released during photosynthesis in the Baltic⁶. All these distributions were determined on the basis of satellite data from the SEVIRI (METEOSAT 9), AVHRR (NOAA 17, 18, 19) and MODIS (AQUA) sensors on 24 April 2011 with the aid of the DESAMBEM algorithm modified as above.

Note that the values of the three forms of energy (spatially integrated along the vertical from the surface to great depths), summarized above in map form (Figure 5) for Baltic waters, characterize the several steps by which solar radiation enters the ecosystem (PAR, PUR and PSR). They are calculated indirectly from satellite data by way of multi-stage calculations. Such calculations can be performed using the light-photosynthesis model, mentioned earlier (e.g. Woźniak et al. 2003a), and the DESAMBEM algorithm, derived from an expanded version of that model (Woźniak et al. 2008, Darecki et al. 2008). In the first step of these calculations, remote sensing data are used in combination with the DESAMBEM or some similar algorithm to calculate the surface concentration of chlorophyll *a* (denoted by $C_a(0) \equiv C_a(z \approx 0)$), which, among other things, provides an indication of the basin's trophicity. In parallel, or alternatively, one can also determine the surface concentrations of other pigments and other constituents of the sea water, various inherent and apparent optical properties of surface waters related to the basin's trophicity, as well as some photosynthetic characteristics of marine plant communities. In subsequent stages of the calculations, the vertical distributions of the magnitudes determined for the surface waters of the basin (i.e. chlorophyll *a* concentration, optical and photosynthetic characteristics) are found. In the final stage, the vertical distributions of the three forms of energy, i.e. $PAR(z)$, $PUR(z)$ and $PSR(z)$, are calculated, which, in turn, are used to work out the overall values of these energies in the water and to determine the distribution of the quantity of oxygen O_2 released during photosynthesis in the basin. Such calculations for the Baltic for 24 April 2011 are exemplified by the maps Figure 5 showing the daily doses of these energies and the daily amounts of oxygen released during photosynthesis.

It is clear from the above that with the DESAMBEM algorithm one can estimate numerous characteristics of the constituents of Baltic water and its optical properties at different depths, which, in consequence, determine the overall distributions of the various forms of energy associated with the

⁶The quantities of this photosynthetically released oxygen were determined approximately on the assumption that during photosynthesis the assimilation of one atom of carbon is accompanied by the evolution of one molecule of oxygen.

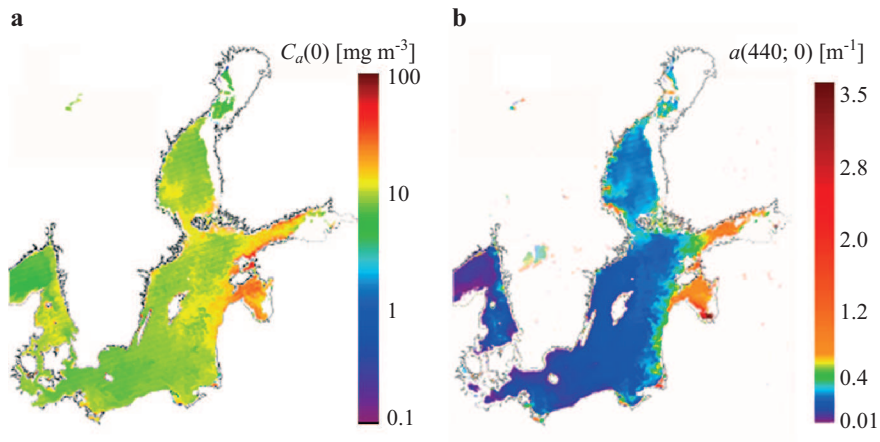


Figure 6. Remotely sensed surface chlorophyll a concentration ($C_a(0) \equiv C_a(z \approx 0)$) and the coefficient of total absorption of light at wavelength 440 nm by dissolved substances and suspended particulate matter in Baltic surface waters $a(440; 0) \equiv a(\lambda = 440 \text{ nm}, z \approx 0)$ on 24 April 2011

successive stages by which solar energy is incorporated into the ecosystem. Because this paper cannot exceed a certain finite length, we cannot present maps of all these characteristics; we have chosen those showing the most important ones, in Figure 6 in this subsection and in Figure 8 in subsection 2.4.

Figure 6 presents maps of the surface chlorophyll a concentration $C_a(0)$ and the coefficient of total absorption of light at wavelength 440 nm by dissolved substances and suspended particulate matter in the sea surface water $a(\lambda = 440 \text{ nm}, z \approx 0) \equiv a(440; 0)$. These parameters are determined from ocean colour analysis based on the MODIS (AQUA) data for 24 April 2011. Values of $C_a(0)$ were calculated using the algorithm presented earlier, *inter alia*, in the paper by Woźniak et al. (2008), while $a(440; 0)$ was calculated with the aid of the formula $a(440 \text{ nm}) = 10^{0.096 - 0.965 \log x}$, where x is the sea's reflectance band ratio for light wavelengths 490 and 665 nm, that is $x = R_{\text{rs}}(490)/R_{\text{rs}}(665)$.

2.3. The radiation balance at the sea surface

The next important application of the methods for remotely sensing marine environmental parameters (indicated in the 'Introduction') that we are testing is their possible use for monitoring processes affecting the quantitative exchange of energy (and also mass) between the sea and the atmosphere (see the right-hand side of Figure 1). As a consequence, these processes lead to the formation of an upward flux of radiation leaving

the Earth, thereby affecting the planet's global energy balance, which has a fundamental influence on its climate. One of the main elements that have to be taken into account in any characterization of this global energy balance is the radiant energy balance, i.e. the balance between the solar short-wave radiation SW at the sea surface (transmitted down and upward) and the long-wave radiation LW (emitted by the sea surface and by the atmosphere); the final balance of these energies is the so-called NET radiation flux. This concept is understood as the following energy difference:

$$NET = (SW_d + LW_d) - (SW_u + LW_u). \quad (1)$$

This is the difference between the total radiant energy flux arriving from the atmosphere at the sea surface ($SW_d + LW_d$), and the total radiant energy flux emitted from the sea surface into the atmosphere ($SW_u + LW_u$). SW_d is the downward solar (short-wave) radiation flux and LW_d is the downward thermal (long-wave) radiation flux of the atmosphere. In contrast, the upward radiation flux ($SW_u + LW_u$) is the sum of short-wave solar radiation flux SW_u reflected upwards from the sea surface (this

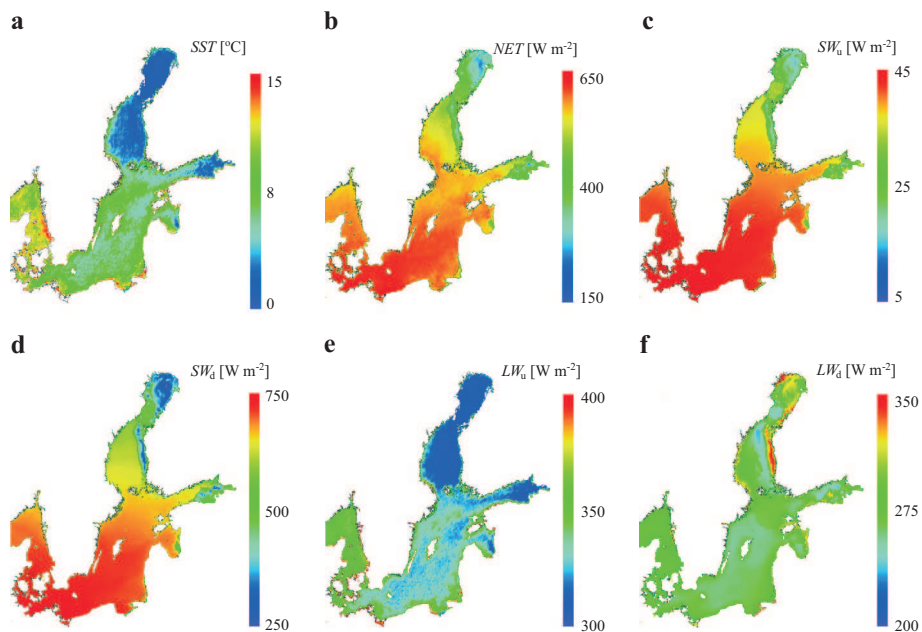


Figure 7. An example of remotely sensed sea surface temperature distributions in the Baltic (a) and the instantaneous NET radiation flux (b), and its corresponding upward and downward components: short-wave – SW_u , SW_d (like downward irradiance $E_{\downarrow S}$ in Fig. 3c) (c, d); long-wave – LW_u , LW_d (e, f), at 11:00 UTC on 24 April 2011 at the Baltic Sea surface

includes radiation emerging from the sea as a result of backscattering within the water) and the long-wave thermal radiation flux emitted by the sea surface LW_u .

Figure 7 (maps b–f) shows the resultant irradiance of the sea surface *NET* radiation flux and its corresponding downward and upward components (short-wave – SW_d , SW_u ; long-wave – LW_d , LW_u). For comparison, the map in Figure 7a shows the distribution of the sea surface temperature *SST*, which bears a strong influence on the *NET* radiation flux, and is the principal input datum for calculating the radiation balance at the sea surface. The distributions of values on these maps were calculated using the algorithms described in Krężel et al. (2008), Zapadka et al. (2008), Woźniak and Krężel (2010) and METEO-FRANCE (2010). The input data for these algorithms were the SEVIRI (MSG) radiometer measurements and data from the prognostic UM weather model.

In the case shown in Figure 7, which refers to the situation in the late morning (11:00 UTC on 24 April 2011), the values of the *NET* radiation flux are positive over the entire Baltic Sea. Nonetheless, this resultant *NET* radiation flux can also take instantaneous negative values. During the daytime the values of this flux are usually positive, because the downward solar radiation flux SW_d is positive. At night, however, the *NET* radiation flux is normally negative, because the long-wave upward radiation flux LW_u , associated with *SST*, is greater than the long-wave downward radiation flux LW_d .

2.4. The optical conditions for the photosynthesis of organic matter and the condition of marine plant communities

As already stated in the Introduction, the DESAMBEM algorithm also makes it possible to estimate indirectly, on the basis of satellite data, a numerous set of spatial distributions of various parameters characterizing the optical conditions for marine photosynthesis, such as the depth of the euphotic zone and the photosynthetic index of the waters, as well as the parameters determining the physiological state (including the condition) of the natural plant communities occurring there. These parameters include the maximum possible assimilation number, the maximum quantum efficiency of photosynthesis and the so-called non-photosynthetic pigment factor. Figure 8 illustrates the spatial distributions of the above-mentioned physiological characteristics of the plant communities and optical conditions in the Baltic Sea as recorded at 11:00 UTC on 24 April 2011.

The first two maps in Figure 8 illustrate the distributions of parameters generally characterizing the photosynthetic predispositions of the Baltic basins. Figure 8a shows the range of the euphotic zone in which photo-

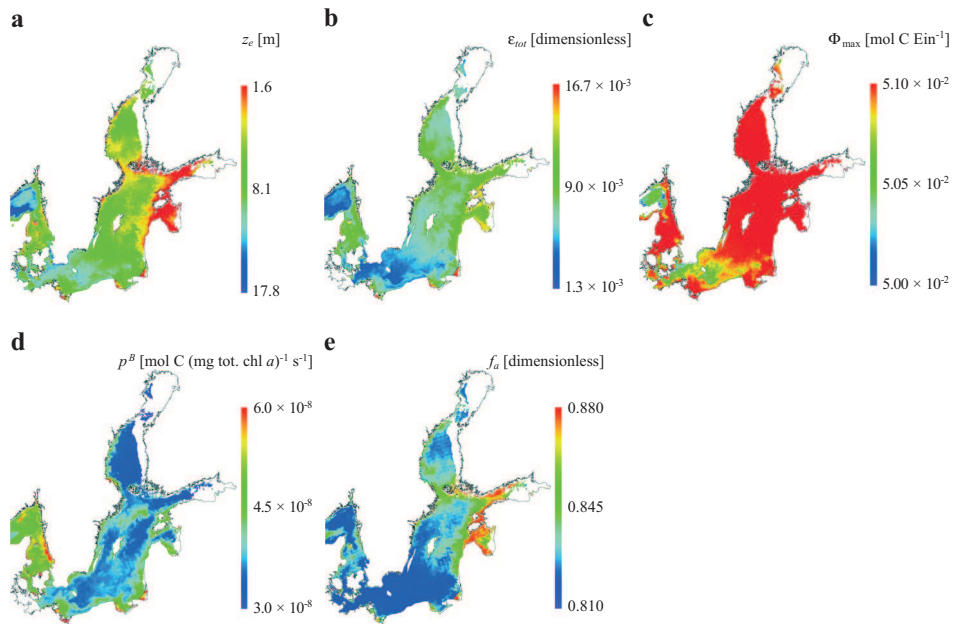


Figure 8. Example maps of remotely sensed distributions in the Baltic Sea at 11:00 UTC on 24 April 2011:

- the depth of the euphotic zone z_e ;
- the photosynthetic index ε_{tot} ;
- the maximum quantum yield of carbon fixation Φ_{max} ;
- the phytoplankton assimilation number P^B ;
- the non-photosynthetic pigment factor f_a

synthesis takes place, calculated according to the optical criterion (the depth to which 1% of the irradiance $PAR(z=0)$ penetrates) with respect to the irradiance crossing the sea surface (see e.g. Woźniak & Dera 2007). Figure 8b shows the distributions of the photosynthetic index in the Baltic, i.e. the parameter defining the part of the solar radiation PAR entering the water that is consumed in the photosynthesis of organic matter. It is thus the ratio of the radiant energy flux consumed in primary production under unit surface area of the water column PSR to the radiant energy flux $PAR(0)$ entering the water.

The next three maps in Figure 8 show the distributions of parameters characterizing in a way the condition of phytoplankton resulting from their physiological state, in particular those parameters describing their potential photosynthetic abilities. Figure 8c shows the distributions of the maximum quantum yield of carbon fixation characteristic of a basin. They define the maximum possible ratios of the number of atoms (or moles) of photosynthetically assimilated carbon to the number (or moles) of quanta of

solar radiation absorbed under given conditions by phytoplankton pigments (Ficek 2001, Ficek et al. 2000). These maximum values are attained at very low irradiances in the sea and are recorded at great depths. The second magnitude characterizing the condition of phytoplankton is the phytoplankton assimilation number – see Figure 8d. This defines the maximum possible rate of photosynthesis in waters of a given trophic type (for a fixed amount of nutrients in those waters and a particular sea water temperature) expressed in numbers of atoms or moles of carbon assimilated in unit time by phytoplankton of unit chlorophyll content. Such maximum rates of photosynthesis are usually recorded at intermediate (photosynthetically optimal) depths, at which irradiance levels are still sufficiently high not to limit the rate of light reactions, yet not so high that destructive photoinhibition of the photosynthetic apparatus comes into play (Majchrowski 2001, Ficek 2001, Woźniak & Dera 2007). In the Baltic such optimal conditions usually (in ca 66% of cases) prevail at depths from 1 to 5 m (see Woźniak et al. 1989). The last of these maps (Figure 8e) shows the distribution of the non-photosynthetic pigment factor, determined for plant communities in Baltic surface waters, that is, in the water layer most exposed to photoinhibitory processes (Woźniak et al. 2007a). Usually ranging in value from 0.5 to 1.0, this parameter is associated with the ratio in plant cells of photosynthetic pigments to the sum of photosynthetic and photoprotecting pigments (the latter are produced by plants under conditions of high irradiance, i.e. under threat of photoinhibition).

2.5. Sea surface temperature *SST* distributions and temperature-associated phenomena in the sea

An important aspect of our work to date aiming to construct an effective SatBałtyk operational system included the successful attempts to expand the applicability of the earlier DESAMBEM algorithms by linking them up with the packet of algorithms from the BALTFOS Forecasting System. The latter are based on forecasting models and procedures for their calibration by the assimilation of satellite data and other data obtained using the diagnostic subalgorithms of the DESAMBEM (see Figure 1 in Part 1 of Woźniak et al. (2011), in this issue). As we have already stated, this is essential in the case of the Baltic, where frequent cloudiness partially or entirely precludes the use of satellite sensors for recording radiation in the visible and thermal infra-red bands for diagnosing various parameters of the marine environment (including chlorophyll concentration and *SST*). In such cases, interpolation (between points in time-space) of measurements remotely sensed in cloud-free areas is often resorted to. Our trials with respect to *SST* interpolations in cloudy areas have shown that such geostatic

methods would not be very effective in an operational system for the Baltic, because of the long periods for which cloudiness persists there. In our opinion, the most effective and reliable approach would be to use data generated by prognostic hydrodynamic and eco-hydrodynamic models, which assimilate data calibrated with data from satellite estimates and/or data generated using the DESAMBEM algorithm.

This is shown by the results of filling in the *SST* map of the Baltic carried out in various ways for 28 April 2009 (11:52 UTC), shown in Figure 9. The *SST* maps are drawn with the aid of a NLSST algorithm (Walton et al. 1998, Krężel et al. 2005) for cloudless areas on the basis of satellite data recorded with an AVHRR sensor (TIROS-N/NOAA). On that day most of the Baltic Sea area was overcast, and estimating SST from satellite data and using diagnostic algorithms was possible for only small areas of the sea (see Figure 9b). The area overcast on that day had been ‘seen’ by the satellite four days earlier, i.e. on 25 April 2009 at 19:15 UTC (see the *SST* distribution in Figure 9a). Kriging interpolation with the aid of linear

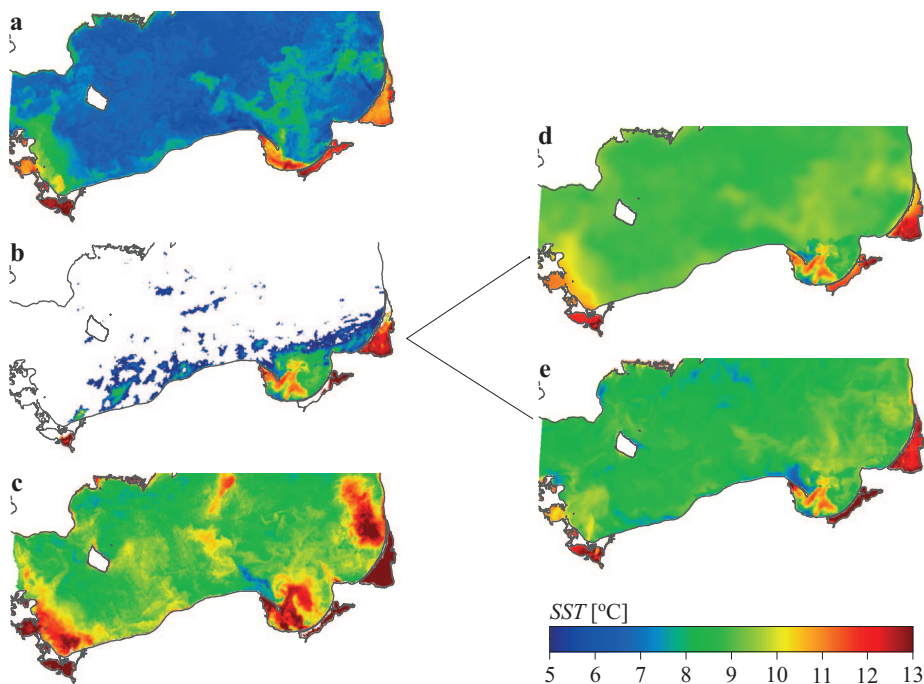


Figure 9. Maps of sea surface temperature distribution in the Baltic Sea plotted according to data from NOAA satellites 17 and 18 for the situation on 25 April 2009, 19:15 UTC (a); 28 April 2009, 11:52 UTC (b); 29 April 2009, 11:42 UTC (c); 28 April 2009, 11:52 UTC – data filled in by kriging (d) and by applying the prognostic hydrodynamic model M3D (e)

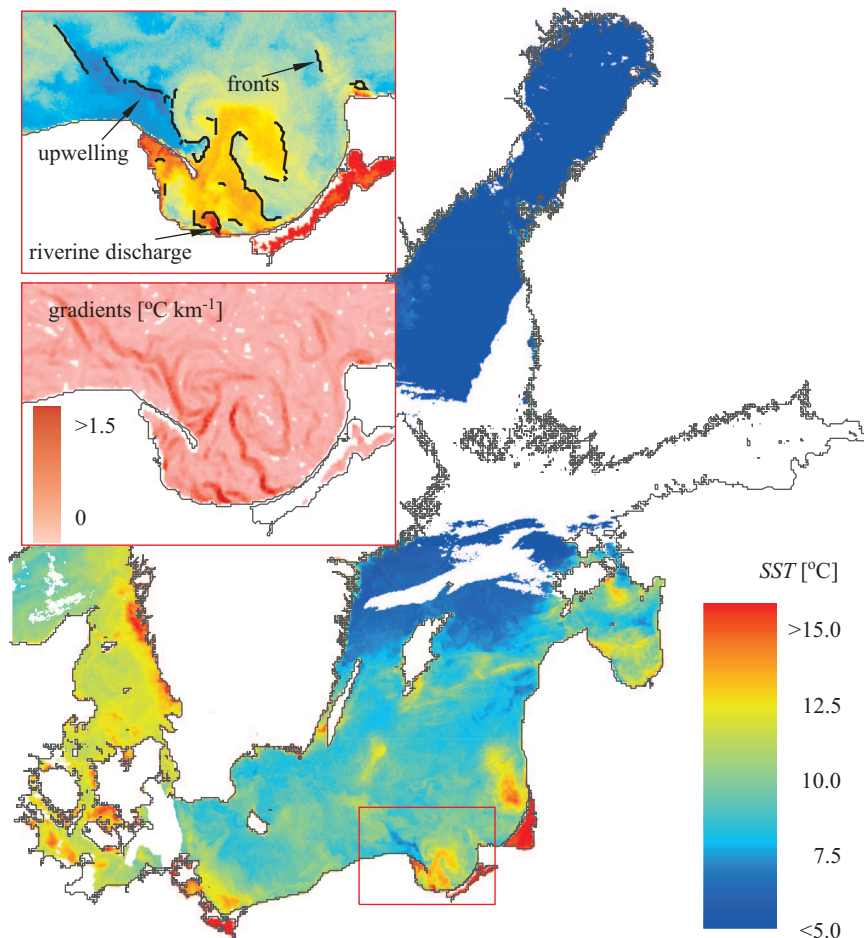


Figure 10. Example of sea surface temperature distribution and its derivatives (maps of temperature gradients and location of thermal fronts), determined on the basis of satellite data for a cloud-free atmosphere at 11:42 UTC on 29 April 2011

regression was applied to these data to make up the missing *SST* data on the cloudy 28 April 2009 (see the *SST* distribution in Figure 9d). Another way of filling in gaps in *SST* fields in overcast areas is to use prognostic models. Figure 9e shows the remotely sensed distribution of *SST* in which overcast areas (Figure 9b) have been replaced by results supplied by the M3D hydrodynamic model (Kowalewski 1997, Kowalewski & Kowalewska-Kalkowska 2011). The *SST* distribution interpolated by kriging (Figure 9d) does not show up the details of the temperature distribution structure and coincides with the results of the next satellite diagnosis (Figure 9c) to a lesser extent than the *SST* distribution obtained with prognostic

modelling (Figure 9e). In particular, the former does not reflect the thermal structures visible in the open part of the sea (for example, the coastal upwelling effect along the Hel peninsula). We can therefore state that prognostic mathematical models estimate data better than statistical methods. This is because these models take into account the physical and other laws governing the spatial distributions of the parameters under scrutiny.

The research results we have achieved so far indicate that our SST distribution maps for the Baltic are also highly suitable for comprehensive oceanological studies. Figure 10 illustrates examples of sea surface temperature (SST) maps and some complex phenomena taking place at sea, identified from these maps, which are usually correlated with temperature distributions. The temperature gradient maps, estimated on the basis of SST maps by means of spatial domain filtration to calculate the gradient towards the maximum local change in SST, were used to identify thermal fronts and subsequently to identify and characterize upwelling events and the extent of spread of terrestrial waters.

3. The prospects for the system's development

As we mentioned earlier, the aims of the SatBałtyk project were not just to diagnose and forecast the structural and functional characteristics of the entire Baltic Sea, but also to predict and record the effects and threats in the sea's shore zone resulting from current and anticipated storm states. To this end, a system has been developed to address such threats to southern Baltic coasts (see Figure 11 for a simplified block diagram). It is founded on the assumptions of and is an extension and modification of the storm early-warning operational system (<http://micore.ztikm.szczecin.pl/>) elaborated by the team of K. Furmańczyk from the University of Szczecin within the framework of the MICORE project, funded from the 7th EU Framework Programme. Essential data for assessing threats to the shore zone with the aid of this system include information on sea levels and wave motion parameters generated by prognostic models, as well as data on shore zone morphology measured in situ. These are the input data for the Xbeach – eXtreme Beach behaviour model. Xbeach is a morphological model with an open source code, originally developed with the financial support of the US Army Corps of Engineers by a consortium consisting of UNESCO-IHE, Deltares (Delft Hydraulics), the Delft University of Technology and the University of Miami. It operates on the two-dimensional propagation of waves, tides, long-term wave action, sediment transport and morphological changes in the shore zone during a storm. The following processes can

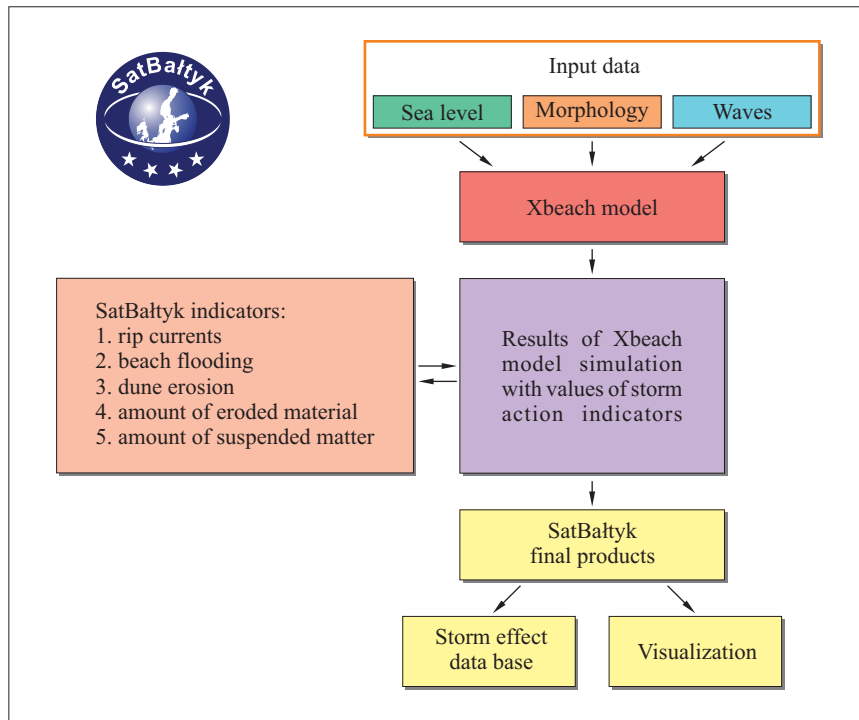


Figure 11. A scheme of the Xbeach system

be modelled: wave breaking, wave run-up (Roelvink et al. 2009), the magnitude of dune erosion, and the magnitude of shore zone erosion. The physical parameters generated by the model are then analysed in the context of the parameters of possible threats, the so-called SatBałtyk indices, defined like the storm effect indices in the MICORE project. The system will predict and visualize indices such as the occurrence of rip currents, the degree of beach inundation and the magnitude of dune erosion, and will enable the amount of material eroded from the shore zone and the quantity of suspended particulate matter in the water to be estimated.

The results of Xbeach model simulations are analysed with the threshold parameters of SatBałtyk indices in order to assess the forecast threat to the shore zone. Apart from the visualization of the forecasts of the several indices on a public website, a ‘storm effect data base’ will also be set up as part of this system. This will store information, which can subsequently be used for making further, more detailed analyses of particular phenomena. A test system is at present being constructed with reference to a 14 km long section of dune shore on the western Polish coast, including the Dziwnów Spit (Figure 12). In later stages of the project, depending on the availability

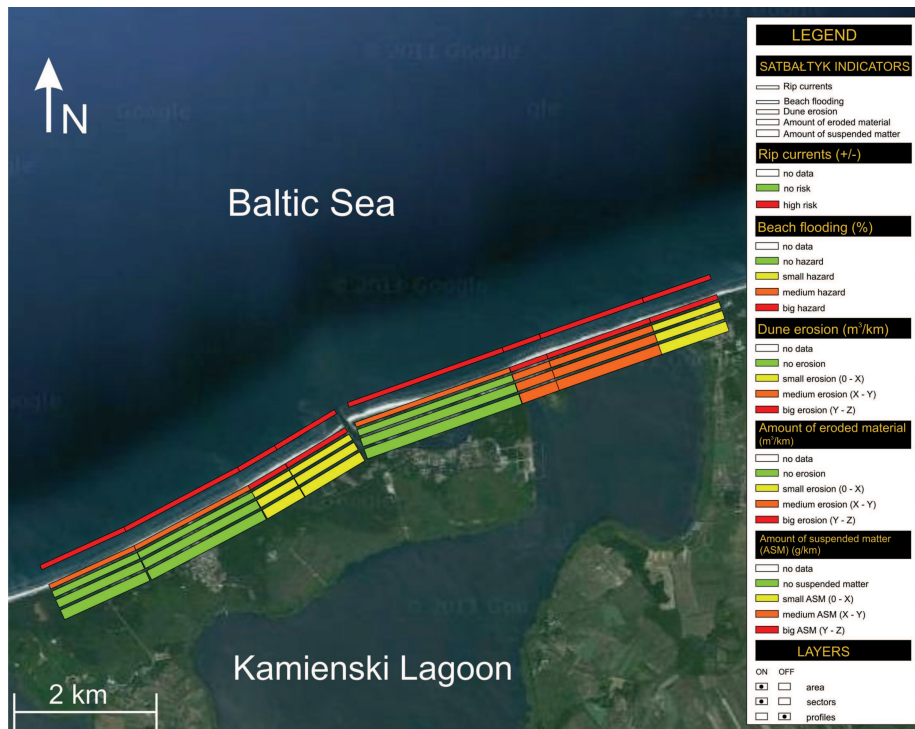


Figure 12. Presentation of the system for recording the effects and threats in the southern Baltic shore zone caused by current and anticipated storm states

of data, it is anticipated that the system will include shore sections along the Lake Kopań Spit, at Sopot and along the Hel Peninsula.

4. Final remarks

We regard the present state of advancement of our work on the construction of the final version of the SatBałtyk Operational System for the remote monitoring of the Baltic Sea as satisfactory. It is already possible to make effective use of this system for estimating current values and for forecasting within a certain range selected biotic and abiotic characteristics of this sea. This has been demonstrated by our research results to date, including our estimates of various characteristics of the Baltic environment given in this article. The preliminary results of the empirical validation of the entire algorithm are described. To this end, the magnitudes of ecosystem parameters determined using the algorithm with data from AVHRR (NOAA 17, 18, 19), SEVIRI (Meteosat 9) and MODIS (AQUA) satellites are compared with the magnitudes of the same parameters recorded at Baltic in situ measurement stations. The relevant

errors have been calculated from these comparisons in accordance with arithmetic and logarithmic statistics (Table 1). At the current stage of

Table 1. Errors in the remotely sensed estimation of selected quantities with the SatBałtyk system at its present stage

Quantity	Arithmetic statistics		Logarithmic statistics			
	Systematic error	Statistical error	Systematic error	Standard error factor	Statistical error	
	$\langle \varepsilon \rangle$ [%]	σ_ε [%]	$\langle \varepsilon \rangle_g$ [%]	x	σ_- [%]	σ_+ [%]
Chl a (C_a)	9.9	± 56.6	-3.2	1.68	-40.5	68.1
E_{1S}	28.7	239	0.650	1.79	-44.4	79.9
daily dose E_{1S}	2.66	1.97	-0.879	1.26	-20.7	26.1
daily dose PAR	2.44	± 23.3	0.24	1.22	-18.3	22.3
daily dose PSR	2.00	± 60.6	-14.6	1.72	-41.7	71.7
	Absolute	Absolute				
	$\langle \varepsilon' \rangle$	σ'_{ε}				
SST	0.37 [°C]	± 1.05 [°C]				
net radiation:						
LW	1 [W m ⁻²]	± 29.7 [W m ⁻²]				
SW	14 [W m ⁻²]	± 38.7 [W m ⁻²]				

Explanation: the above errors in the satellite estimates are given in accordance with the principles of arithmetic and logarithmic statistics and denote (where $X_{i,M}$ – measured magnitudes; $X_{i,C}$ – estimated magnitudes):

absolute mean error (systematic): $\langle \varepsilon' \rangle = N^{-1} \sum_i \varepsilon'_i$ (where $\varepsilon'_i = (X_{i,C} - X_{i,M})$),

mean relative error (systematic): $\langle \varepsilon \rangle = N^{-1} \sum_i \varepsilon_i$ (where $\varepsilon_i = (X_{i,C} - X_{i,M})/X_{i,M}$),

standard deviation (statistical error) of ε' : $\sigma'_{\varepsilon} = \sqrt{\frac{1}{N} \left(\sum (\varepsilon'_i - \langle \varepsilon' \rangle)^2 \right)}$,

standard deviation (statistical error) of ε : $\sigma_{\varepsilon} = \sqrt{\frac{1}{N} \left(\sum (\varepsilon_i - \langle \varepsilon \rangle)^2 \right)}$,

mean logarithmic error: $\langle \varepsilon \rangle_g = 10^{\langle \log(X_{i,C}/X_{i,M}) \rangle} - 1$,

standard error factor: $x = 10^{\sigma_{\log}}$,

statistical logarithmic errors: $\sigma_+ = x - 1$, $\sigma_- = \frac{1}{x} - 1$.

development of the SatBałtyk algorithm for the Baltic, these errors, typical of remote, spatial estimates, can be regarded as fairly satisfactory. Nevertheless, in order to reduce them, improvement of all the components of this complex algorithm will continue.

This series of two papers presents only the possibilities of investigations of Baltic environment with the use SatBałtyk operational system. In the paper were described the exemplary results for selected situations mainly

for April 2011. The analyses of seasonal changes of different parameters of Baltic ecosystem are in progress and will be presented soon.

References

- Bird R.E., Riordan C., 1986, *Simple solar spectral model for direct and diffuse irradiance on horizontal and tilted planes at the Earth's surface for cloudless atmospheres*, J. Clim. Appl. Meteorol., 25 (1), 87–97.
- Darecki M., Ficek D., Krężel A., Ostrowska M., Majchrowski R., Woźniak S.B., Bradtke K., Dera J., Woźniak B., 2008, *Algorithms for the remote sensing of the Baltic ecosystem (DESAMBEM). Part 2: Empirical validation*, Oceanologia, 50 (4), 509–538.
- Darula S., Kittler R., Gueymard C. A., 2005, *Reference luminous solar constant and solar luminance for illuminance calculations*, Sol. Energy, 79 (5), 559–565.
- Dera J., Woźniak B., 2010, *Solar radiation in the Baltic Sea*, Oceanologia, 52 (4), 533–582.
- Ficek D., 2001, *Modelling the photosynthesis quantum yield in various marine basins*, Diss. and monogr., 14, IO PAS, Sopot, 224 pp., (in Polish).
- Ficek D., Majchrowski R., Ostrowska M., Kaczmarek S., Woźniak B., Dera J., 2003, *Practical applications of the multi-component marine photosynthesis model (MCM)*, Oceanologia, 45 (3), 395–423.
- Ficek D., Majchrowski R., Ostrowska M., Woźniak B., 2000, *Influence of non-photosynthetic pigments on the measured quantum yield of photosynthesis*, Oceanologia, 42 (2), 231–242.
- Gueymard C. A., 2004, *The sun's total and spectral irradiance for solar energy applications and solar radiation models*, Sol. Energy, 76 (4), 423–453.
- Keevallik S., Loitjäär K., 2010, *Solar radiation at the surface in the Baltic Proper*, Oceanologia, 52 (4), 583–597.
- Kowalczyk P., Zabłocka M., Sagan S., Kuliński K., 2010, *Fluorescence measured in situ as a proxy of CDOM absorption and DOC concentration in the Baltic Sea*, Oceanologia, 52 (3), 431–471.
- Kowalewski M., 1997, *A three-dimensional, hydrodynamic model of the Gulf of Gdańsk*, Oceanol. Stud., 26 (4), 77–98.
- Kowalewski M., Kowalewska-Kalkowska H., 2011, *Performance of operationally calculated hydrodynamic forecasts during storm surges in the Pomeranian Bay and Szczecin Lagoon*, Boreal Environ. Res., 16 (Suppl. A), 27–41.
- Krężel A., 1985, *Solar radiation at the Baltic Sea surface*, Oceanologia, 21, 5–32.
- Krężel A., 1997, *A model of solar energy input to the sea surface*, Oceanol. Stud., 26 (4), 21–34.
- Krężel A., Kozłowski Ł., Paszkuta M., 2008, *A simple model of light transmission through the atmosphere over the Baltic Sea utilising satellite data*, Oceanologia, 50 (2), 125–146.

- Kreżel A., Paszkuta M., 2011, *Automatic detection of cloud cover over the Baltic Sea*, J. Atmos. Ocean. Tech., 28 (9), 1117–1128.
- Kreżel A., Szymanek L., Kozłowski Ł., Szymelfenig M., 2005, *Influence of coastal upwelling on chlorophyll a concentration in the surface water along the Polish coast of the Baltic Sea*, Oceanologia, 47 (4), 433–452.
- Majchrowski R., 2001, *Influence of irradiance on the light absorption characteristics of marine phytoplankton*, Stud. i rozpr., 1, Pom. Akad. Pedagog., Słupsk, 131 pp., (in Polish).
- Majchrowski R., Stoń-Egiert J., Ostrowska M., Woźniak B., Ficek D., Lednicka B., Dera J., 2007, *Remote sensing of vertical phytoplankton pigment distributions in the Baltic: new mathematical expressions. Part 2. Accessory pigment distribution*, Oceanologia, 49 (4), 491–511.
- METEO-FRANCE, 2010, *Algorithm theoretical basis document for cloud products*, Météo-France/Centre de Météorologie Spatiale.
- Neckel H., Labs D., 1981, *Improved data of solar spectral irradiance from 0.33 to 1.25 μm* , Sol. Phys., 74 (1), 231–249.
- Ostrowska M., Majchrowski R., Stoń-Egiert J., Woźniak B., Ficek D., Dera J., 2007, *Remote sensing of vertical phytoplankton pigment distributions in the Baltic: new mathematical expressions. Part 1: Total chlorophyll a distribution*, Oceanologia, 49 (4), 471–489.
- Roelvink D., Reniers A., van Dongeren A., van Thiel de Vries J., McCall R., Lescinski J., 2009, *Modelling storm impacts on beaches, dunes and barrier islands*, Coast. Eng., 56 (11–12), 1133–1152, doi:10.1016/j.coastaleng.2009.08.006.
- Rozwadowska A., 2004, *Optical thickness of stratiform clouds over the Baltic inferred from on-board irradiance measurements*, Atmos. Res., 72 (1–4), 129–147, doi:10.1016/j.atmosres.2004.03.012.
- Rozwadowska A., 2007, *Influence of aerosol vertical profile variability on retrievals of aerosol optical thickness from NOAA AVHRR measurements in the Baltic region*, Oceanologia, 49 (2), 165–184.
- Rozwadowska A., Isemer H.-J., 1998, *Solar radiation fluxes at the surface of the Baltic Proper. Part 1. Mean annual cycle and influencing factors*, Oceanologia, 40 (4), 307–330.
- Spencer J. W., 1971, *Fourier series representation of the position of the Sun*, Search, 2 (5), 172 pp.
- Walton C. C., Pichel W. G., Sapper J. F., May D. A., 1998, *The development and operational application of nonlinear algorithms for the measurement of sea surface temperatures with the NOAA polar-orbiting environmental satellites*, J. Geophys. Res., 103 (C12), 27 999–28 012, doi:10.1029/98JC02370.
- Woźniak B., 1985, *Elements of photosynthetic energetics in the southern Baltic*, [in:] *Utilisation of solar energy in the photosynthesis process of the Black and Baltic Sea phytoplankton*, O. I. Koblentz-Mishke, B. Woźniak & Yu. E. Ochakovskiy (eds.), Inst. Okeanol. AN SSSR, Moscow, 205–230, (in Russian).

- Woźniak B., Bradtke K., Darecki M., Dera J., Dudzińska-Nowak J., Dzierzbicka-Głowacka L., Ficek D., Furmańczyk K., Kowalewski M., Krężel A., Majchrowski R., Ostrowska M., Paszkuta M., Stoń-Egiert J., Stramska M., Zapadka T., 2011, *SatBaltyk – A Baltic environmental satellite remote sensing system – an ongoing project in Poland. Part 1: Assumptions, scope and operating range*, in this issue.
- Woźniak B., Dera J., 2007, *Light absorption in sea water*, Springer, New York, 454 pp.
- Woźniak B., Dera J., Ficek D., Majchrowski R., Ostrowska M., Kaczmarek S., 2003a, *Modelling light and photosynthesis in the marine environment*, *Oceanologia*, 45 (2), 171–245.
- Woźniak B., Ficek D., Ostrowska M., Majchrowski R., Dera J., 2007a, *Quantum yield of photosynthesis in the Baltic: a new mathematical expression for remote sensing applications*, *Oceanologia*, 49 (4), 527–542.
- Woźniak B., Hapter R., Dera J., 1989, *Light curves of marine phytoplankton photosynthesis in the Baltic*, *Oceanologia*, 27, 61–78.
- Woźniak B., Krężel A., Darecki M., Woźniak S.B., Majchrowski R., Ostrowska M., Kozłowski Ł., Ficek D., Olszewski J., Dera J., 2008, *Algorithm for the remote sensing of the Baltic ecosystem (DESAMBEM). Part 1: Mathematical apparatus*, *Oceanologia*, 50 (4), 451–508.
- Woźniak B., Majchrowski R., Ostrowska M., Ficek D., Kunicka J., Dera J., 2007b, *Remote sensing of vertical phytoplankton pigment distributions in the Baltic: new mathematical expressions. Part 3: Non-photosynthetic pigment absorption factor*, *Oceanologia*, 49 (4), 513–526.
- Woźniak B., Rozwadowska A., Kaczmarek S., Woźniak S.B., Ostrowska M., 2003b, *Seasonal variability of the solar radiation flux and its utilisation in the Southern Baltic*, ICES Coop. Res. Rep. No. 257, 280–298.
- Woźniak M., Krężel A., 2010, *Sea surface temperature retrieval from MSG/SEVIRI data in the Baltic Sea area*, *Oceanologia*, 52 (3), 331–344.
- Zapadka T., Krężel A., Woźniak B., 2008, *Long-wave radiation budget at the Baltic Sea surface from satellite and atmospheric model data*, *Oceanologia*, 50 (2), 147–166.

Annex 1

Abbreviations

Abbreviation	Explanation
1	2
AOP	Apparent optical properties of the basin
AOT	Aerosol optical thickness
APT	The Automatic Picture Transmission (APT) system provides a reduced resolution data stream from the AVHRR instrument. Any two of the six available AVHRR channels can be chosen by ground command for processing and ultimate output to the APT transmitter. The analogue APT signal is transmitted continuously and can be received in real time by relatively unsophisticated, inexpensive ground station equipment
AVHRR	The Advanced Very High Resolution Radiometer is a broad-band, four, five or six channel (depending on the model) scanner, sensing in the visible, near-infrared, and thermal infrared portions of the electromagnetic spectrum. This sensor is carried on the National Oceanic and Atmospheric Administration's (NOAA's) Polar Orbiting Environmental Satellites (POES), beginning with TIROS-N in 1978
AVHRR/NOAA	AVHRR working on board a Tiros-N/NOAA series spacecraft (satellite). AVHRR (NOAA 14) – AVHRR working on board the NOAA 14 satellite
BALTFOS	BALTic FOrcasting System
BOOS	Baltic Operational Oceanographic System
CICE	The Los Alamos sea ice model. 'CICE' – an acronym, for 'Community Ice Code'. The acronym is pronounced 'sea ice'
3DCEMBS	3 Dimensional Coupled Ecosystem Model of the Baltic Sea
DESAMBEM	Complex satellite algorithm for the Baltic, also known as the DESAMBEM Diagnostic System (abbreviation taken from the name of previous project No. PBZ-KBN 056/P04/2001) 'The Development of a Satellite Method for Baltic Ecosystem Monitoring'
DMSP	Defense Meteorological Satellites Program (DMSP) – a series of spacecraft to investigate the Earth's environment from an altitude of ~ 800 km. They were all put into Sun-synchronous near-polar orbits (inclination ~ 99 degrees). Of interest to the high-energy science community are DMSP F10, F11, F12, F13, F14, F15, F16, F17 and F18

Abbreviations (*continued*)

1	2
EcoSat	A new model (EcoSat) enabling the assimilation of remotely determined distributions of surface chlorophyll <i>a</i> concentration
ENVISAT	ENVISAT (ENVironmental SATellite) – the largest Earth Observation spacecraft ever built. It carries ten sophisticated optical and radar instruments to provide continuous observation and monitoring of the Earth's land, atmosphere, oceans and ice caps. Launched in 2002
EOS/AQUA	Aqua is a NASA Earth Science satellite mission named for the large amount of information that the mission will be collecting about the Earth's water cycle. The Aqua mission is a part of the NASA-centered international Earth Observing System (EOS)
GMES	Global Monitoring for Environment and Security – the European Programme for the establishment of a European capacity for Earth Observation
HRPT	The High Resolution Picture Transmission (HRPT) system provides data from all spacecraft instruments at a rate of 665.400 bps. The S-band realtime transmission consists of the digitized unprocessed output of five AVHRR/3 channels, plus the TIP (HIRS/3 for NOAA KLM and HIRS/4 on NOAA-N, -P, SBUV/2, SEM, DCS/2) data and AMSU data. All information necessary to calibrate the instrument outputs is included in the data stream
ICM	Interdisciplinary Centre for Mathematical and Computational Modelling, Warsaw University – http://www.icm.edu.pl/eng/
IF PUnS	Institute of Physics of the Pomeranian University in Słupsk
IMCS US	Institute of Marine and Coastal Sciences of the Szczecin University
Interkosmos	The Soviet space programme of the late 1960s and 1970s and 1980s
IOPAN	Institute of Oceanology of the Polish Academy of Sciences
IOP	Inherent optical properties of the basin
IOUG	Institute of Oceanography, University of Gdańsk
IR	Infrared radiation
METEOSAT	Geostationary meteorological satellites operated

Abbreviations (*continued*)

1	2
	by EUMETSAT under the Meteosat Transition Programme (MTP) and the Meteosat Second Generation (MSG) program
MICORE Project	Morphological Impacts and COastal Risks induced by Extreme storm events - Framework Programme (www.micore.eu)
MNiSW	Ministry of Science and Higher Education (Poland)
MODIS/AQUA	The MODerate-resolution Imaging Spectroradiometer (MODIS) is a payload scientific instrument launched into Earth orbit by NASA in 2002 on board the AQUA (EOS PM) satellite
MSG (currently METEOSAT 9)	Meteosat Second Generation (MSG) is a significantly enhanced, follow-on system to the previous generation of Meteosat (MFG). MSG consists of a series of four geostationary meteorological satellites that will operate consecutively
N, P	Nutrients: nitrate, phosphorus
NLSST	Nonlinear algorithm for sea surface temperature retrieval from AVHRR/NOAA data
NOAA	National Oceanic and Atmospheric Administration of the USA
PAR	Photosynthetic Available Radiation – the radiation in the spectral range ca 400–700 nm
POM	Princeton Ocean Model, developed by Prof. G. Mellor and Dr. A. F. Blumberg at Princeton University at the end of the 1970s
POP	Parallel Ocean Program
PP	Primary production
ProDeMo	Production and Destruction of Organic Matter Model – a 3-dimensional coupled hydrodynamic-ecological model
PSR	Photosynthetically Stored Radiation
PUR	Photosynthetically Utilized Radiation
SatBałtyk	The research project ‘Satellite Monitoring of the Baltic Sea Environment’ (2010–2014)
SBOS	SatBałtyk Operational System
SeaWiFS/OrbView 2	Sea-viewing Wide Field-of-view Sensor. Radiometer working on board the OrbView-2 (AKA SeaStar) satellite
SEVIRI	Spinning Enhanced Visible and Infrared Imager.

Abbreviations (*continued*)

1	2
	Radiometer working on board the METEOSAT satellite
SMHI	Swedish Meteorological and Hydrological Institute
SST	Sea Surface Temperature
TIROS-N/NOAA	National Oceanic and Atmospheric Administration's (NOAA's) Polar Orbiting Environmental Satellites (POES), beginning with TIROS-N in 1978
UM	Unified Model – numerical weather prediction model developed by the United Kingdom Met Office
UV	UV – ultraviolet radiation
WRF	Weather Research and Forecasting Model

Annex 2

Symbols

Symbol	Explanation	Unit
1	2	3
$a_{pl}(z)$	Coefficient of light absorption by phytoplankton in a water column at any depth z (vertical distribution of a_{pl})	m^{-1}
$C_a(0)$	Chlorophyll a concentration in the surface water layer	mg m^{-3}
$C_a(z)$	Chlorophyll a concentration in the water column at any depth z (vertical distribution of C_a)	mg m^{-3}
$C_i(z)$	Concentration of the i -th pigment in the water column at any depth z (vertical distribution of C_i)	mg m^{-3}
E	Irradiance	W m^{-2}
$E_{\downarrow OA}$	Downward solar irradiance on a flat horizontal surface at the top of the atmosphere	W m^{-2}
$E_{\downarrow S}$	Downward solar irradiance at the sea surface	W m^{-2}
$E_{\downarrow OS}$	Downward solar irradiance reaching the sea surface through a cloudless atmosphere	W m^{-2}
$E_d(\lambda, z)$	Downward irradiance of wavelength λ in the water column at any depth z (vertical distribution of spectral E_d)	W m^{-2}
ICE	Ice cover area	m^2
$K_d(\lambda)$	Downward irradiance attenuation coefficient	m^{-1}
LW_d	Downward long-wave radiation flux at the sea surface	W m^{-2}
LW_u	Upward long-wave radiation flux at the sea surface	W m^{-2}
NET	Net radiation flux (sea surface radiation balance)	W m^{-2}
O_2	Daily quantity of oxygen O_2 released during photosynthesis in the water column	$\text{g m}^{-2} \text{day}^{-1}$
$PAR(z)$	Downward irradiance in the PAR spectral range in the water column at any depth z (vertical distribution of PAR irradiance)	W m^{-2}
PSR	The energy incorporated into the ecosystem (i.e. primary production) in energy units in the water column under unit sea surface area during unit time	$\text{J m}^{-2} \text{s}^{-1}$ and $\text{MJ m}^{-2} \text{day}^{-1}$
$PSR(z)$	The energy incorporated into the ecosystem (i.e. primary production) in energy units in unit volume of water at any depth z during unit time	$\text{J m}^{-3} \text{s}^{-1}$ and $\text{MJ m}^{-3} \text{day}^{-1}$
PUR	Photosynthetically utilized radiation energy in the water column under unit sea surface area	$\text{J m}^{-2} \text{s}^{-1}$ and

Symbols (*continued*)

1	2	3
	during unit time	$\text{MJ m}^{-2} \text{ day}^{-1}$
$PUR(z)$	Photosynthetically utilized radiation energy in unit volume of water at any depth z during unit time (i.e. vertical distribution of radiation energy absorbed by phytoplankton pigments)	$\text{J m}^{-3} \text{ s}^{-1}$ and $\text{MJ m}^{-3} \text{ day}^{-1}$
$P(z)$	Primary production in unit volume of water at any depth z during unit time (vertical distribution of primary production)	$\text{gC m}^{-3} \text{ day}^{-1}$
P_{tot}	Total primary production in the water column under unit sea surface area during unit time	$\text{gC m}^{-2} \text{ day}^{-1}$
SST	Sea surface temperature	$^{\circ}\text{C}$
SW_{d}	Downward short-wave radiation flux at the sea surface	W m^{-2}
SW_{u}	Upward short-wave radiation flux at the sea surface	W m^{-2}